An intercellular polyamine transfer via gap junctions regulates proliferation and response to stress in epithelial cells

Bénédicte Desforges, Patrick Curmi, Ouissame Bounedjah, Samir Nakib, Loic Hamon, Jean-Pascal de Bandt, David Pastre

An intercellular polyamine transfer via gap junctions regulates proliferation and response to stress in epithelial cells

Bénédicte Desforges[a], Patrick A. Curmi[a], Ouissame Bounedjah[a], Samir Nakib[b], Loic Hamon[a], Jean-Pascal De Bandt[b,c], and David Pastré[a]

[a]Institut National de la Santé et de la Recherche Médicale, UMR829, Laboratoire Structure-Activité des Biomolécules Normales et Pathologiques, Université Evry-Val d'Essonne, Evry 91025, France; [b]Service de Biochimie, AP-HP Hôpitaux Universitaires Paris Centre, 75679 Paris, France; [c]Laboratoire de Biologie de la Nutrition, EA4466, Département de Biologie Expérimentale, Métabolique et Clinique, Faculté de Pharmacie, Université Paris-Descartes, 75270 Paris, France

ABSTRACT **In the organism, quiescent epithelial cells have the potential to resume cycling as a result of various stimuli, including wound healing or oxidative stress. Because quiescent cells have a low polyamine level, resuming their growth requires an increase of their intracellular polyamine levels via de novo polyamine synthesis or their uptake from plasma. Another alternative, explored here, is an intercellular exchange with polyamine-rich cycling cells via gap junctions. We show that polyamines promote gap junction communication between proliferating cells by promoting dynamical microtubule plus ends at the cell periphery and thus allow polyamine exchange between cells. In this way, cycling cells favor regrowth in adjacent cells deprived of polyamines. In addition, intercellular interactions mediated by polyamines can coordinate the translational response to oxidative stress through the formation of stress granules. Some putative in vivo consequences of polyamine-mediated intercellular interactions are also discussed regarding cancer invasiveness and tissue regeneration.**

Monitoring Editor
Carl-Henrik Heldin
Ludwig Institute for Cancer Research

Received: Oct 10, 2012
Revised: Jan 31, 2013
Accepted: Mar 12, 2013

INTRODUCTION

Natural polyamines, that is, divalent putrescine, trivalent spermidine, and tetravalent spermine, are small cationic organic molecules present in the millimolar range in mammalian cells and are necessary for cell proliferation (Tabor and Tabor, 1984; Thomas and Thomas, 2001), in line with their higher concentration in cancer cells compared with normal cells (Heby, 1981; Pegg, 2009). Polyamines, as major counterions of negatively charged nucleic acids (RNA and DNA to a lesser extent; Watanabe *et al.*, 1991), exert their proliferative effect via the expression of growth-related genes (Celano *et al.*, 1989), the stimulation of protein synthesis (Nishimura *et al.*, 2005; Landau *et al.*, 2010), and more specifically the hypusination of eIF5A (Jakus *et al.*, 1993). Polyamines can either be transported from the extracellular environment (Seiler *et al.*, 1996) or directly produced in cells by a complex set of enzymes devoted to their synthesis or degradation (Casero and Pegg, 1993; Moinard *et al.*, 2005). Their intracellular concentration is regulated via an enzymatic feedback involving in particular ornithine decarboxylase (ODC), the rate-limiting enzyme in the polyamine biosynthetic pathway, and antizime (AZ), which negatively regulates ODC activity and thus the polyamine content via finely tuned polyamine-dependent ribosomal frameshifting (Coffino, 2001).

Quiescent eukaryotic cells have significantly reduced ODC activity and lower intracellular polyamine concentration than their proliferating counterparts (Heby *et al.*, 1973, 1975; Kramer *et al.*, 2001). The switch between quiescence and proliferation thus requires cells to either resume polyamine synthesis or increase their active transport (Heby *et al.*, 1973; Celano *et al.*, 1988; Bello-Fernandez *et al.*, 1993; Satriano *et al.*, 2001). However, an alternative pathway can also be put forward for adherent cells: an exchange of polyamines from cell to cell through gap junctions. This hypothesis makes sense

This article was published online ahead of print in MBoC in Press (http://www.molbiolcell.org/cgi/doi/10.1091/mbc.E12-10-0729) on March 20, 2013.

Address correspondence to: David Pastré (david.pastre@univ-evry.fr).

Abbreviation used: Pu, putrescine.

Treatment (6 d)	Putrescine (fmol/cell ×10)	Spermidine (fmol/cell ×10)	Spermine (fmol/cell ×10)
Control (subconfluent)	1.4 ± 0.4	18.9 ± 0.6	12.6 ± 0.9
DFMO (0.5 mM) + APCHA (100 μM) (subconfluent)	0.22 ± 0.2	5.7 ± 1.5	4.6 ± 1.2
DFMO (0.5 mM) + APCHA (100 μM) + wash with Pu (60 μM) (24 h) (subconfluent)	4.8 ± 1.8	25.9 ± 1.1	9.3 ± 6.2
DFMO (0.5 mM) + APCHA (100 μM) + wash without Pu (24 h) (subconfluent)	<0.1	5.7 ± 0.36	2.1 ± 0.1
Agmatine (0.5 mM) (subconfluent)	0.3 ± 0.13	<0.05	5 ± 1.2
Agmatine (0.5 mM) + wash with Pu (60 μM) (24 h) (subconfluent)	3.1 ± 1.4	22 ± 11	7.4 ± 2.4
Control (quiescent)	0.3 ± 0.1	3.5 ± 1.7	5.3 ± 1.3
DFMO (0.5 mM) + APCHA (100 μM) (quiescent)	0.14 ± 0.09	4.2 ± 0.8	4.8 ± 2.7
Agmatine (0.5 mM) (quiescent)	0.22 ± 0.01	1.9 ± 0.4	6.1 ± 1.4

TABLE 1: Intracellular polyamine concentration in NRK cells after indicated treatments.

if we consider the scarce presence of polyamines in plasma compared with the intracellular pool (being in the micromolar range for extracellular putrescine and spermidine, the major polyamines in plasma; Russell and Russell, 1975; Shipe *et al.*, 1979; Kwon *et al.*, 2004; and in the millimolar range for intracellular spermidine and spermine; Watanabe *et al.*, 1991). In addition, due to their small size (Veenstra, 1996)—only 88 Da for putrescine—and hydrophilic nature (Weber *et al.*, 2004), polyamines satisfy all the requirements to be transported from cell to cell via gap junctions. However, adherent cells are not necessarily connected through gap junction plaques (Pepper *et al.*, 1989; van Zoelen and Tertoolen, 1991). One factor that favors the transport and maintenance of gap junction plaques is the presence of microtubules at the cell/cell interface (Lauf *et al.*, 2002). Connexin proteins like Cx43 can directly interact with microtubules (Giepmans *et al.*, 2001) or indirectly via the microtubule plus end–binding protein EB1 (Shaw *et al.*, 2007). In that respect, columnar quiescent cells mostly display stable microtubules, which are bundled and aligned along the apical–basolateral axis (Bacallao *et al.*, 1989; Musch, 2004), leaving little chance for dynamical microtubules to interact at the cell/cell interface with gap junctions, if any, whereas proliferating cells mostly display many dynamical microtubules at the cell/cell interface, a better configuration for gap junction maintenance and communication.

To address these points, we analyze the role played by polyamines in microtubule dynamics in normal rat kidney cells (NRK cells) deprived of polyamines. We demonstrate that natural polyamines are important for the proper maintenance of gap junction communications by their promotion of microtubule dynamics and that cycling cells have the potential to resume the proliferation of neighboring polyamine-depleted cells due to polyamine transfer through gap junctions. We also consider two interesting consequences of the exchange of polyamines among gap junction-connected cells. First, we explore the putative coordinated response to stress among gap junction–connected cells. Polyamines regulate the formation of mRNA stress granules (Li *et al.*, 2010), which participate in the reprogramming of the translational machinery during stress (Kedersha *et al.*, 2005; Arimoto *et al.*, 2008; Chernov *et al.*, 2009). A collective translational response associated with stress granules may then take place, provided that intercellular communications ensure a homogeneous distribution of polyamines in epithelia. Second, we consider the role of the polyamine sharing via gap junctions during wound healing. Indeed, both polyamines (McCormack *et al.*, 1992, 1993; Witte and Barbul, 2003) and gap junction communications (Gabbiani *et al.*, 1978; Goliger and Paul, 1995; Qiu *et al.*, 2003) play a key role during wound healing. In particular, gap junction plaques generally appear in the wounded area, whereas they are barely present away from it (Spanakis *et al.*, 1998; Desforges *et al.*, 2011). Finally, we advance some possible consequences of polyamine-mediated intercellular signalization for normal or abnormal proliferative patterns in vivo, especially during wound healing, tissue regeneration, and cancer and for the global response of epithelia to oxidative stress exposure.

RESULTS

We analyze the effect of intracellular polyamines on the cytoskeleton of NRK cells by using either difluoro-methylornithine (DFMO), an inhibitor of ODC (Meyskens and Gerner, 1999), combined with *N*-(3-aminopropyl)cyclohexylamine (APCHA), an inhibitor of spermine synthase (Beppu *et al.*, 1995), or agmatine alone, the decarboxylation product of arginine (Lortie *et al.*, 1996), which inhibits polyamine synthesis (Satriano *et al.*, 1998). Long treatments (6 d) were necessary to decrease significantly all polyamine levels (Table 1) and especially the trivalent spermidine and tetravalent spermine levels, which promote microtubule assembly (Mechulam *et al.*, 2009; Savarin *et al.*, 2010). Such treatments are cytostatic, as NRK cells were arrested but resumed growing after polyamine supplementation. During this transition, global gene expression is modified, and this accounts most probably for the results when comparing polyamine-depleted cell and proliferating cells.

Polyamines organize the cell cytoskeleton

In agreement with previous reports (McCormack *et al.*, 1999; Ray *et al.*, 2003), intracellular polyamine depletion led to the appearance of large actin stress fibers at the cell cortex (Figure 1A), along with a flattened shape of subconfluent cells (Supplemental Figure S1A). Cells also displayed reduced microtubule extensions toward the cell/cell interface (Figure 1A). In agreement with this, the number of growing microtubule plus ends reaching the cell/cell interface is significantly reduced after polyamine depletion (Figure 1B and Supplemental Figure S2). Addition of putrescine to the culture medium of

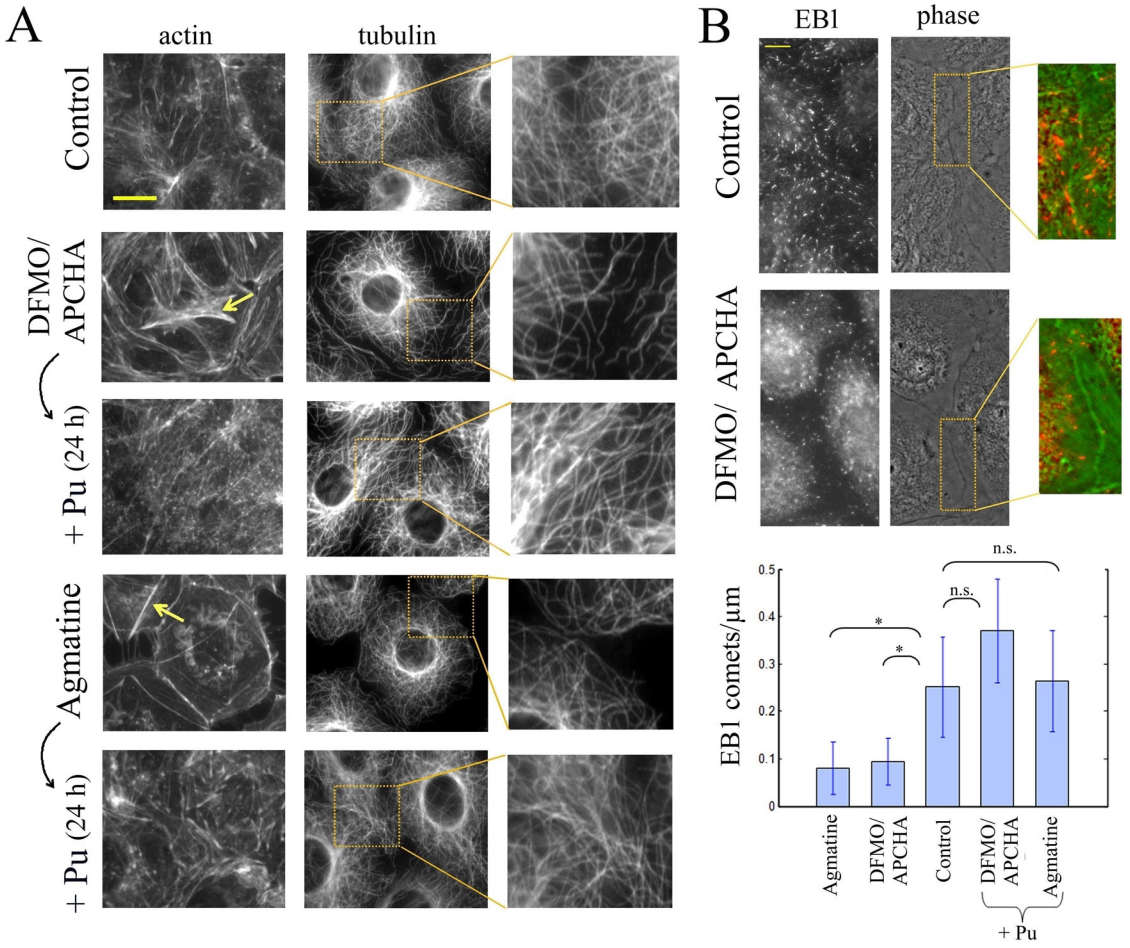

FIGURE 1: Polyamine depletion in NRK cells leads to the presence of thick actin stress fibers and limited extensions of the microtubule network at the cell cortex. (A) NRK cells were untreated or treated with 0.5 mM DFMO and 100 µM APCHA or 500 µM agmatine for 6 d and supplemented or not with 60 µM putrescine (Pu) during the following day (see *Materials and Methods*). Both DFMO/APCHA and agmatine treatments induced the appearance of stress fibers at the cell cortex (arrows), which were no longer observed after putrescine supplementation. In addition, as shown in higher-magnification images, microtubule extensions toward cell/cell interface were scarce after DFMO/APCHA and agmatine treatments and recovered after putrescine supplementation. Scale bar, 15 µm. (B) After indicated treatments, NRK cells were labeled with anti-EB1 to detect the growing microtubule plus ends. Phase contrast microscopy was used to observe the cell/cell interface (top; scale bar, 10 µm). The higher-magnification images show that DFMO/APCHA-treated cells displayed fewer EB1 comets at the cell/cell interface compared with control. Merge image: EB1 (red) and inverted phase microscopy image (green). Statistical analysis of the number of EB1 comets reaching the cell/cell interface per micrometer, as described in Supplemental Figure S2 (bottom). Results are mean ± SD obtained on five different samples. *$p < 0.05$ by *t* test. n.s., not significant.

polyamine-depleted cells led to the replenishment of intracellular polyamine pool (Table 1) and the restoration of normal microtubule extensions (Figure 1, A and B). To demonstrate that this recovery was specific to natural polyamines and not due to an electrostatic effect on cell adhesion or cell membrane, we added divalent agmatine instead of divalent putrescine after the DFMO/APCHA treatment. In this case, we observed no recovery of the microtubule extensions (Supplemental Figure S3). In both polyamine-depleted and putrescine-supplemented cells, large actin stress fibers at the cell cortex can also be observed after inhibition of Rac1, a small Rho GTPase that, when inactivated, leads to the appearance of actin stress fibers at the cell cortex (Tapon and Hall, 1997; Ray *et al.*, 2003). However, they are not seen after the inhibition of Rho-associated kinase, which leads to Rac1 activation (Supplemental Figure S1B), even in polyamine-depleted cells. This indicates that Rac1 inactivation most probably induces the appearance of actin stress fibers at the cell cortex in polyamine-depleted cells (McCormack *et al.*, 1999; Ray *et al.*, 2003). When cycloheximide was added to block de novo protein synthesis simultaneously with putrescine to replenish the polyamine pool in polyamine-depleted cells, we noticed a significant regrowth of microtubules from the centrosome (Supplemental Figure S3), so that protein synthesis by polyamines cannot alone account for microtubule regrowth.

Polyamines and gap junction communications

The overall effect of polyamines on the epithelial cell cytoskeleton raised interesting issues regarding the consequences for intercellular interactions. After DFMO/APCHA treatment, fewer gap junction plaques were observed compared with control cells (Figure 2A). We may then assume that polyamines favor the formation of gap junction plaques. However, in apparent contradiction with this assumption, agmatine treatment, although leading also to polyamine

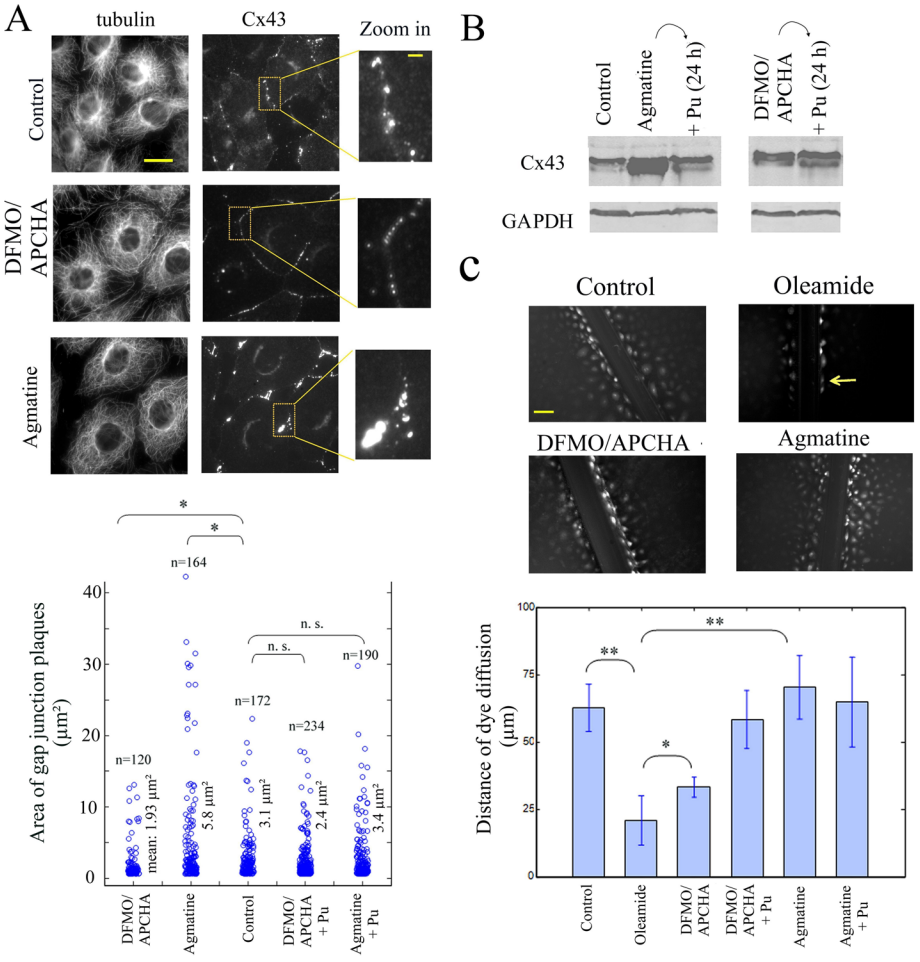

FIGURE 2: Gap junction communications in polyamine-depleted cells. (A) NRK cells were labeled with anti-tubulin and anti-Cx43 antibodies after the indicated treatments for 6 d. As shown in higher-magnification images, compared with control cells, DFMO/APCHA-treated cells displayed small gap junction plaques, whereas agmatine-treated cells formed thick gap junction plaques. Incubation with 60 μM putrescine (Pu) for the last day allowed the recovery of smaller gap junction plaques in agmatine-treated cells and thicker plaques in DFMO/APCHA-treated cells. Scale bar, 15 μm. Statistical analysis of the area of gap junction plaques was performed using ImageJ software. Scatter plots show results obtained on *n* plaques. **p* < 0.05 by *t* test over the null hypothesis that the two population means are equal. n.s., not significant. (B) Western blotting indicates that agmatine increased the expression level of Cx43. DFMO/APCHA treatment did not change the Cx43 expression level. GAPDH was used as a loading control. (C) The transfer of Lucifer yellow, a small hydrophilic dye, from cell to cell was observed after indicated treatments using the scrape-loading procedure. Long-range dye transfer via gap junction communications was detected in both agmatine- and DFMO/APCHA-treated cells, even though slightly reduced after the latter treatment. As control, 50 μM of the gap junction inhibitor oleamide for 2 h strongly inhibited gap junction communication and, in this case, only cells at the vicinity of the wound appeared bright (arrow). Scale bar, 80 μm. Statistical analysis of dye diffusion through gap junctions was performed as described in Supplemental Figure S4. Results are mean ± SD obtained on five different areas. ***p* < 0.005; **p* < 0.05 by *t* test.

depletion, induced the formation of larger gap junction plaques at the cell/cell interface than in control cells (Figure 2A). This is further confirmed by Western blotting, where agmatine but not DFMO/APCHA treatment indeed led to an overexpression of Cx43, this pattern being reversed by putrescine supplementation (Figure 2B). A closer look at the gap junctions formed in the presence of agmatine revealed particularly thick plaques, raising doubts about whether such gap junction plaques were functional. To answer this question, we performed scrape-loading assays (el-Fouly *et al.*, 1987) to probe the transfer of LY dye between cells via gap junctions and found that agmatine-treated cells can indeed efficiently communicate via gap junctions. Given that DFMO/APCHA-treated cells also displayed long-range dye transfer compared with oleamide-treated cells (Figure 2C and Supplemental Figure S4), polyamine depletion is thus not associated with an impairment of gap junction communications. However, the large size of gap junction plaques of agmatine-treated cells may reflect impaired maintenance.

Impaired microtubule dynamics and maintenance of gap junctions in polyamine-depleted cells

To investigate whether polyamines regulate gap junction organization through their action on microtubule dynamics, we first examined whether disruption of microtubules per se (using nocodazole) could lead to mislocated gap junctions in control or DFMO/APCHA-treated cells. We found after nocodazole treatment (5 μM for the last 24 h) the presence of abundant connexin-rich vesicles in the cytosol of both cells, in agreement with impaired transport (Supplemental Figure S5A). In both polyamine-supplemented and depleted cells, after Taxol treatment (100 nM for the last 24 h), which abolishes microtubule dynamics, the presence of connexin was observed at the cell/cell interface, but large gap junction plaques tended to disappear as if microtubule dynamics allowed the higher-order assembly of gap junction proteins. In agmatine-treated cells (Figure 2A), we hypothesized that the observed thick gap junction plaques may result from an impaired microtubule-related transport of connexins. To explore this idea, we disrupted gap junction plaques by the reversible inhibitor oleamide (50 μM; Guan *et al.*, 1997) and observed their reformation 90 min after its removal (Figure 3, A and B). Connexin aggregates were reformed in agmatine-treated cells, but most of them were not located at the cell/cell interface but instead in the bulk cytoplasm, in contrast with putrescine-supplemented cells, which displayed a proper location of small gap junction plaques (Figure 3B and Supplemental Figure S5B). The poor reformation of gap junction plaques in agmatine-treated cells may then result from an impairment of microtubule function. In agreement with this, microtubule disruption by nocodazole after oleamide removal similarly led to mislocated connexin-rich vesicles in the bulk cytoplasm of agmatine-treated cells that were supplemented with putrescine, as observed with agmatine-treated cells in the absence of nocodazole.

These results prompted us to further investigate the role of polyamines on the elongation rate of dynamical microtubule plus ends. Videomicroscopy of EB1 revealed that the elongation rate of

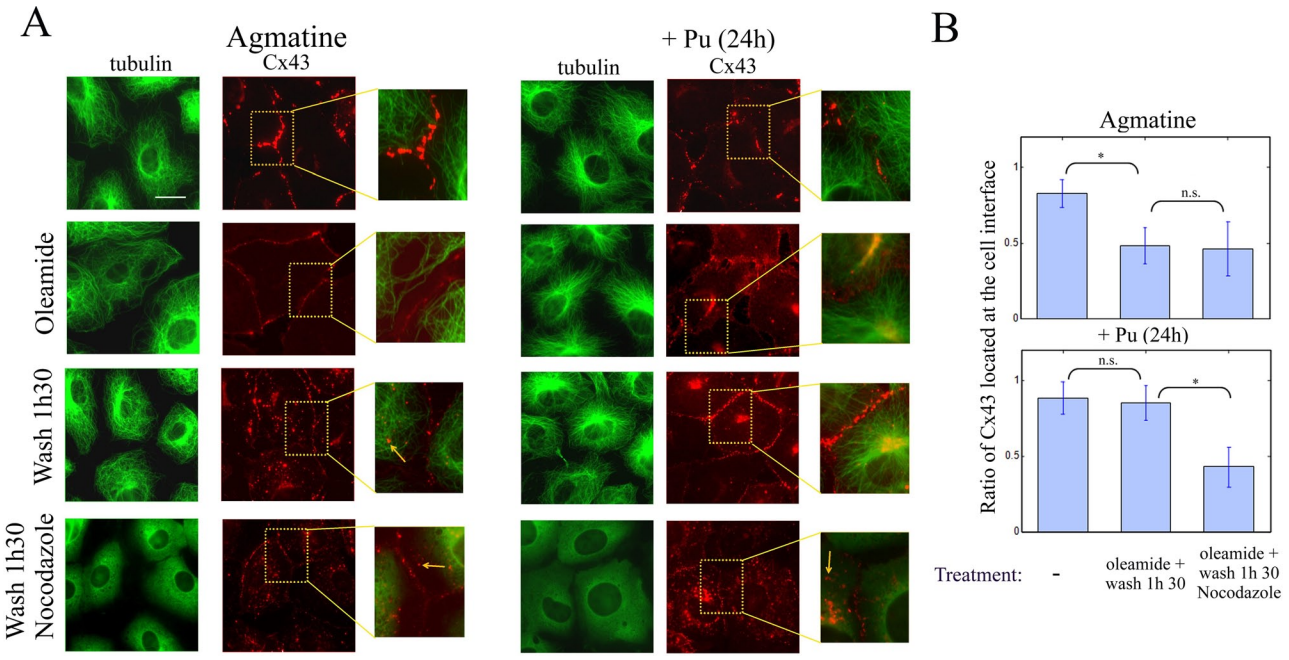

FIGURE 3: Microtubules are necessary for the proper assembly of gap junction plaques after putrescine supplementation in polyamine-depleted cells. (A) Gap junctions of agmatine-treated cells, supplemented or not with putrescine, were disrupted using 50 μM oleamide for 2 h, and their reassembly was observed after its removal for 90 min. NRK cells were then labeled with anti-tubulin (green) and anti-Cx43 (red). Agmatine-treated cells displayed many connexin aggregates in the cytoplasm after oleamide washout (arrow). In contrast, proper location of the newly reformed small gap junction plaques was observed in putrescine-supplemented cells. Microtubule disruption by 5 μM nocodazole during the recovery period inhibited the reformation of gap junctions at the cell/cell interface even after putrescine treatment (see improper cytoplasmic location indicated by arrows). Scale bar, 15 μm. (B) Statistical measurement of the ratio of gap junction plaque area located at the interface to that in the cytoplasm. Results are mean ± SD from 100 plaques on three different samples. *$p < 0.05$ by *t* test. n.s., not significant (see Supplemental Figure S5B for an example showing how this ratio was estimated). No difference in this ratio was observed between agmatine-treated cells and putrescine-supplemented cells (*t* test not significant) before the treatment with oleamide.

microtubules and the number of dynamical plus ends at the cell cortex were considerably reduced as a result of polyamine depletion after both DFMO/APCHA and agmatine treatments (Figure 4, A and B, and Supplemental Videos S1–S3). Again, polyamine-depleted cells could recover dynamical microtubules at the cell cortex after putrescine supplementation. A similar pattern was obtained after staining of endogenous EB1. Some of the microtubule ends appeared to directly target gap junction plaques, whereas very few dynamical microtubules appeared to be in close proximity to gap junction plaques in polyamine-depleted cells (Figure 4C).

Intercellular interactions between control and polyamine-depleted cells trigger a switch from quiescence to proliferation

To probe whether polyamines can transmit a signal to control proliferation, we considered the putative interaction of polyamine-depleted NRK cells with overlaid control NRK cells, that is, polyamine-rich proliferating cells in coculture assays (see *Materials and Methods*). As a prerequisite, we performed a series of control experiments, with the following results. 1) In the absence of overlaid control cells, DFMO/APCHA-treated cells after 6 d were unable to resume proliferation after DFMO and APCHA removal, provided that the culture medium was not supplemented with putrescine; 2) polyamine levels remained low in the DFMO/APCHA-treated cells under such conditions (Table 1); 3) extracellular putrescine, however, allowed them to resume proliferation (Figure 5A), indicating that they were not irreversibly arrested; 4) finally, we tested whether agmatine-treated cells remained quiescent after agmatine washout and observed that they could reenter the cell cycle even if this occurred with a significant delay, probably because agmatine does not directly target ODC but instead activates antizyme (Satriano *et al.*, 1998).

From these observations, we therefore chose to use the DFMO/APCHA-treated cells for coculture experiments (Figure 5B). When control cells were overlaid on subconfluent DFMO/APCHA-treated cells, a significant number of the previously polyamine-depleted cells became bromodeoxyuridine (BrdU) positive after 36 h (Figure 5C). Regrowth was also clearly observed after 4 d, thus allowing multiple divisions (Supplemental Figure S6). Clusters of polyamine-depleted cells free of overlaid control cells did not resume proliferation (Supplemental Figure S7A). Because we also detected the presence of gap junctions at the interface between polyamine-depleted and control cells (Supplemental Figure S7B), we then explored the involvement of gap junction communications in the regrowth of polyamine-depleted cells using oleamide. In the same cell cluster, the inhibition of gap junction communications by oleamide (50 μM) reduced BrdU incorporation and proliferation of DFMO/APCHA-treated cells but not that of control cells (Figure 5, B and C, and Supplemental Figure S6). Because oleamide by itself does not inhibit the regrowth of polyamine-depleted cells after putrescine supplementation (Figure 5A), the blockage of gap junction communications by oleamide was probably responsible for the partial

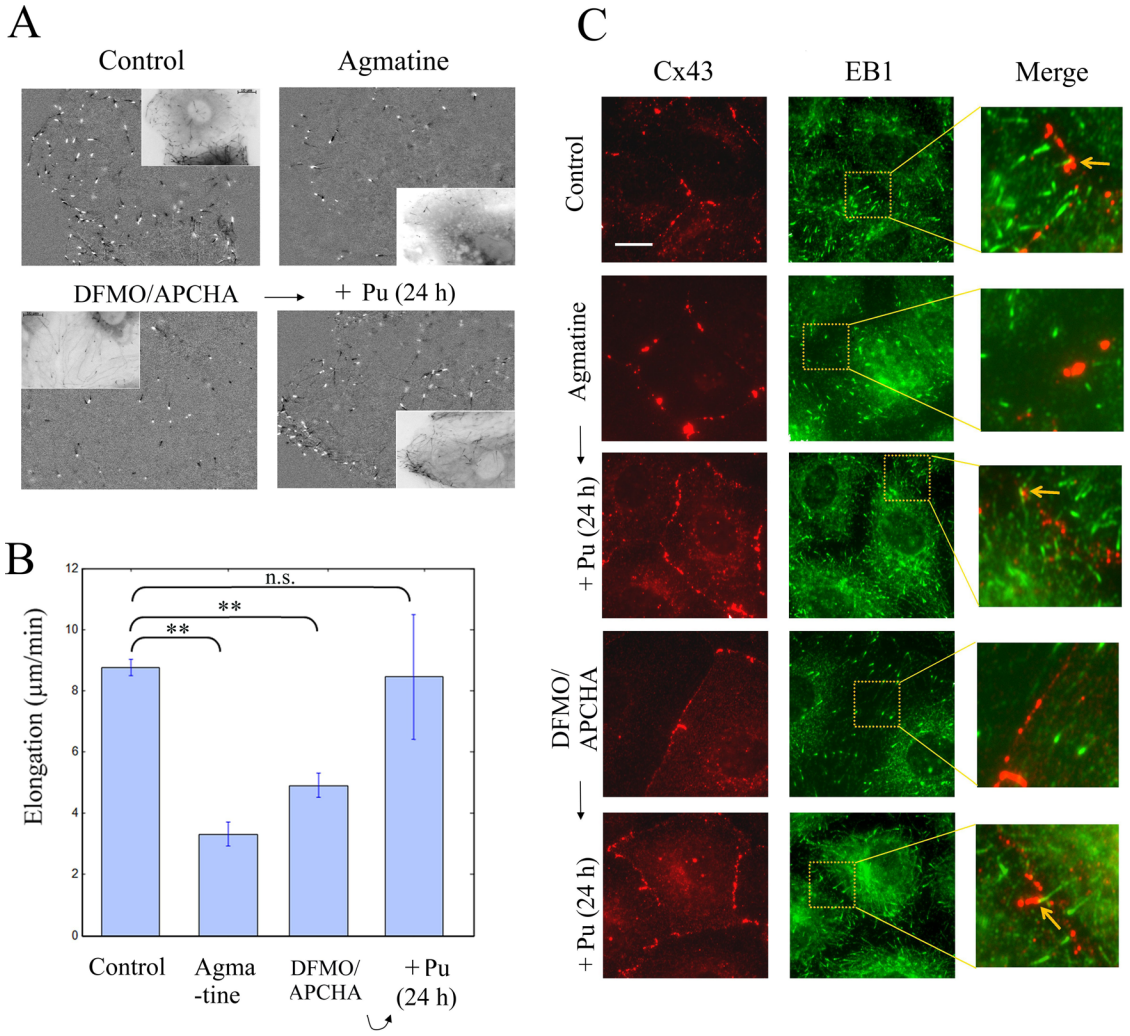

FIGURE 4: Dynamical microtubule plus ends target gap junction plaques in putrescine-supplemented cells, in contrast with polyamine-depleted cells. (A) Microtubule dynamics was revealed in transfected NRK cells using GFP-EB1 via differential images obtained by subtracting two consecutive images in a time-lapse series (first image, black microtubule plus ends [see insets]; second image after 8 s, white microtubule plus ends). Stable microtubules were then invisible, whereas microtubule dynamics (elongation or shrinkage) led to the appearance of black (initial position) and white (final position) dots. The results show that many more dynamical microtubules were detected at the cell cortex in control and putrescine-supplemented cells than in polyamine-depleted cells. Scale bar, 15 µm. See also Supplemental Videos S1–S3. (B) Quantitative measurements of microtubule elongation rates in transfected NRK cells determined by analyzing time-lapse videos of GFP-EB1. The elongation rates were significantly slower in the absence of intracellular polyamines than in control or putrescine-supplemented cells. Results are mean ± SD. $^{**}p < 0.005$ by *t* test. n.s., not significant. (C) NRK cells labeled with anti-EB1 (green) and anti-Cx43 (red) were treated as indicated for 6 d. As shown in higher-magnification images, polyamine-depleted cells displayed only few dynamical microtubule plus ends at the cell periphery, which were not in the vicinity of gap junction plaques, whereas in control and putrescine-supplemented cells (60 µM for the last day), many more microtubule plus ends were observed, and some of them were in close proximity to gap junction plaques (arrows).

inhibition of polyamine-depleted cell proliferation after the interaction with control cells. Another point that we explored is whether polyamine-depleted cells can resume growth after interacting with control cells by de novo intracellular polyamine production and (or) their transit from control cells. To distinguish between these two options, we kept DFMO in the culture medium after the overlay of control cells to prevent polyamine synthesis (Figure 5C). Because control cells treated with DFMO generally continue dividing for at least 2 d in vitro (Nishimura *et al.*, 2002), they have enough polyamines to trigger cell division of polyamine-depleted cells, and, indeed, we observed that the regrowth of polyamine-depleted cells was again detected (Figure 5C), although DFMO reduced the proportion of BrdU-positive cells of DFMO/APCHA-treated cells.

Polyamine-depleted NRK cells display impaired stress granule assembly upon arsenite exposure

We then explored the potential consequence of polyamine sharing among gap junction–connected cells in the translational response to stress mediated by stress granules, as their assembly is polyamine dependent (Li *et al.*, 2010). To confirm this dependence, we analyzed whether polyamine-depleted cells were able to form mRNA stress granules after arsenite-induced stress. In NRK cells, both

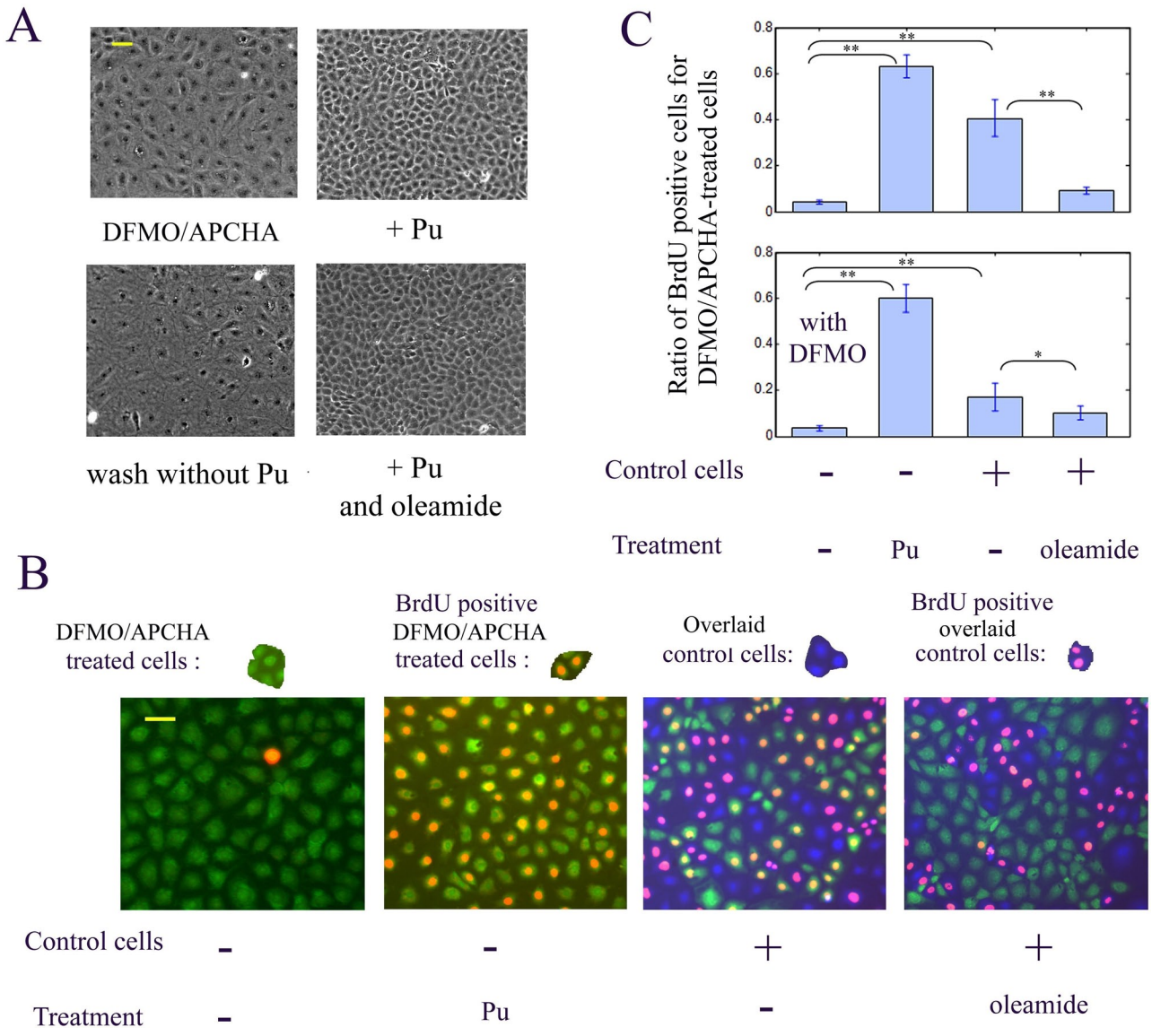

FIGURE 5: DFMO/APCHA-treated cells resume growing after interacting with control cells. (A) Phase contrast microscopy indicates that NRK cells treated with DFMO/APCHA for 6 d did not resume growing even if DFMO and APCHA were removed for 48 h. The addition of putrescine (60 μM) during 48 h after the DFMO and APCHA removal led to a significant proliferation. This was also observed in the presence of oleamide (50 μM). Scale bar, 100 μm. (B) Control cells were overlaid on subconfluent NRK cells treated with DFMO/APCHA for 6 d and allowed to interact for 36 h in the absence of DFMO and APCHA and under indicated conditions. Control cells were stained blue with CMAC, and DFMO/APCHA-treated cells were stained green with CFMDA. The incorporation of BrdU in the nucleus after BrdU exposure for the last 6 h was detected with anti-BrdU (red). BrdU-positive cells appeared with a pink nucleus for control cells and a yellow nucleus for previously DFMO/APCHA-treated cells. The presence of control cells increased the ratio of BrdU-positive cells among DFMO/APCHA-treated cells. In the presence of oleamide, DFMO/APCHA-treated cells displayed fewer yellow nuclei, in contrast with control cells, which displayed many pink nuclei. Scale bar, 15 μm. (C) Statistical measurement of BrdU incorporation after cells were allowed to interact under indicated conditions in the presence or absence of DFMO to inhibit polyamine synthesis. The presence of DFMO reduced cell proliferation in DFMO/APCHA-treated cells when interacting with control cells, but the increase of the ratio of BrdU-positive cells among DFMO/APCHA-treated cells remained significant. Results are mean ± SD from 400 cells on three different samples. $^{**}p < 0.005$, $^{*}p < 0.05$ by *t* test.

DFMO/APCHA and agmatine treatments led to the unambiguous inhibition of stress granule assembly after induction of stress by a 45-min exposure to 0.5 mM arsenite (Figure 6A), which is in agreement with a previous report (Li *et al.*, 2010). In addition, we observed that restoration of polyamine pool by putrescine supplementation of polyamine-depleted NRK cells was associated with a restored ability to form stress granules under arsenite exposure (Figure 6A). To examine the role of intercellular exchange, we then proceeded to the same coculture assays as before with control cells overlaid on DFMO/APCHA-treated cells in the absence of extracellular polyamines. The results (Figure 6B) showed that the arsenite-induced formation of stress granules took place in

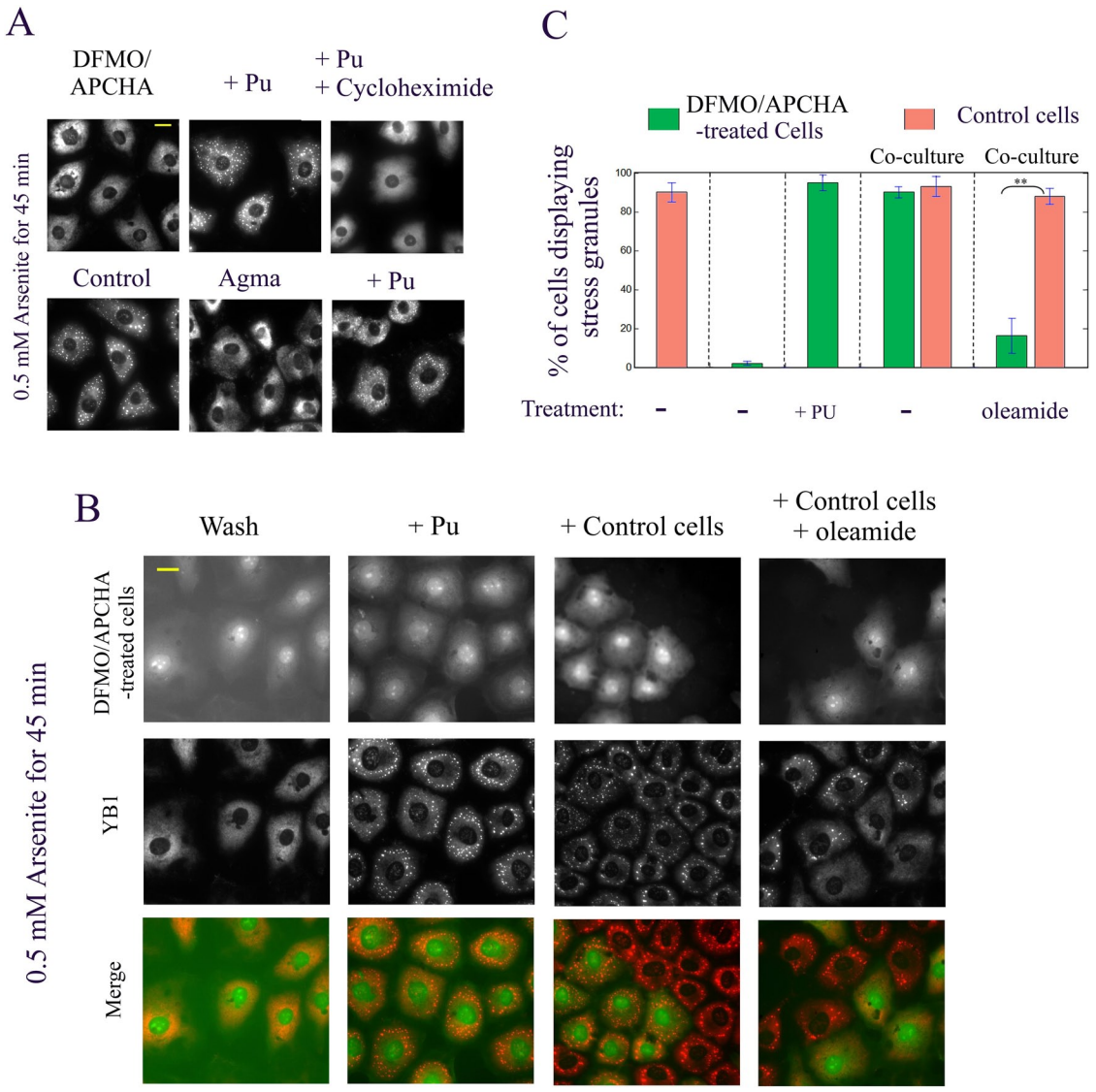

FIGURE 6: Intercellular interactions control the formation of stress granules. (A) NRK cells were exposed to 0.5 mM arsenite for 45 min after indicated treatments for 6 d, and YB1 labeling was used to detect stress granules formed in the cytoplasm. Agmatine or DFMO/APCHA treatment impaired the formation of stress granules, but this effect was reversed in putrescine-supplemented cells (60 μM for 24 h). Cycloheximide (10 μg/ml for 1 h before and during arsenite exposure), which stabilizes polysomes and thus inhibits stress granule formation, was used as control to indicate that we truly observed stress granules in NRK cells. Scale bar, 10 μm. (B) Control cells were overlaid on subconfluent NRK cells treated with DFMO/APCHA for 6 d and allowed to interact for 36 h in the absence of DFMO and APCHA and under indicated conditions. DFMO/APCHA-treated cells were stained green with CFMDA. Stress granules were then detected after arsenite exposure via YB1 labeling. DFMO/APCHA-treated cells retrieved their ability to form stress granules after interacting with control cells. Within the same cluster, oleamide inhibited stress granule assembly in DFMO/APCHA-treated cells but not in control cells. Scale bar, 15 μm. (C) Statistical measurements of stress granule formation under the same conditions as B. Results are mean ± SD from 400 cells on three different samples. $^{**}p < 0.005$ by *t* test.

DFMO/APCHA-treated cells when interacting with control cells (Figure 6, B and C). Of interest, in the presence of oleamide to block gap junction communications, stress granule formation was impaired in DFMO/APCHA-treated but not in control cells (Figure 6B).

Quiescent cells have low polyamine levels and cannot form stress granules

Quiescent NRK cells were obtained by allowing them to reach confluence followed by a 9-d contact inhibition. To ascertain that the cells were quiescent, we controlled their BrdU negativity, columnar organization, and the presence of cilia. Polyamine content in these cells was significantly reduced and similar to that observed after DFMO/APCHA treatment (Table 1). Of interest, even if treated with DFMO/APCHA or agmatine, quiescent cell polyamine content cannot be further decreased (Table 1). Owing to the low intracellular concentration of polyamines in quiescent cells, we wondered whether arsenite-induced stress granule formation could be observed in these conditions. Our results showed that the formation of large stress granules was impaired, with only dot-like granules

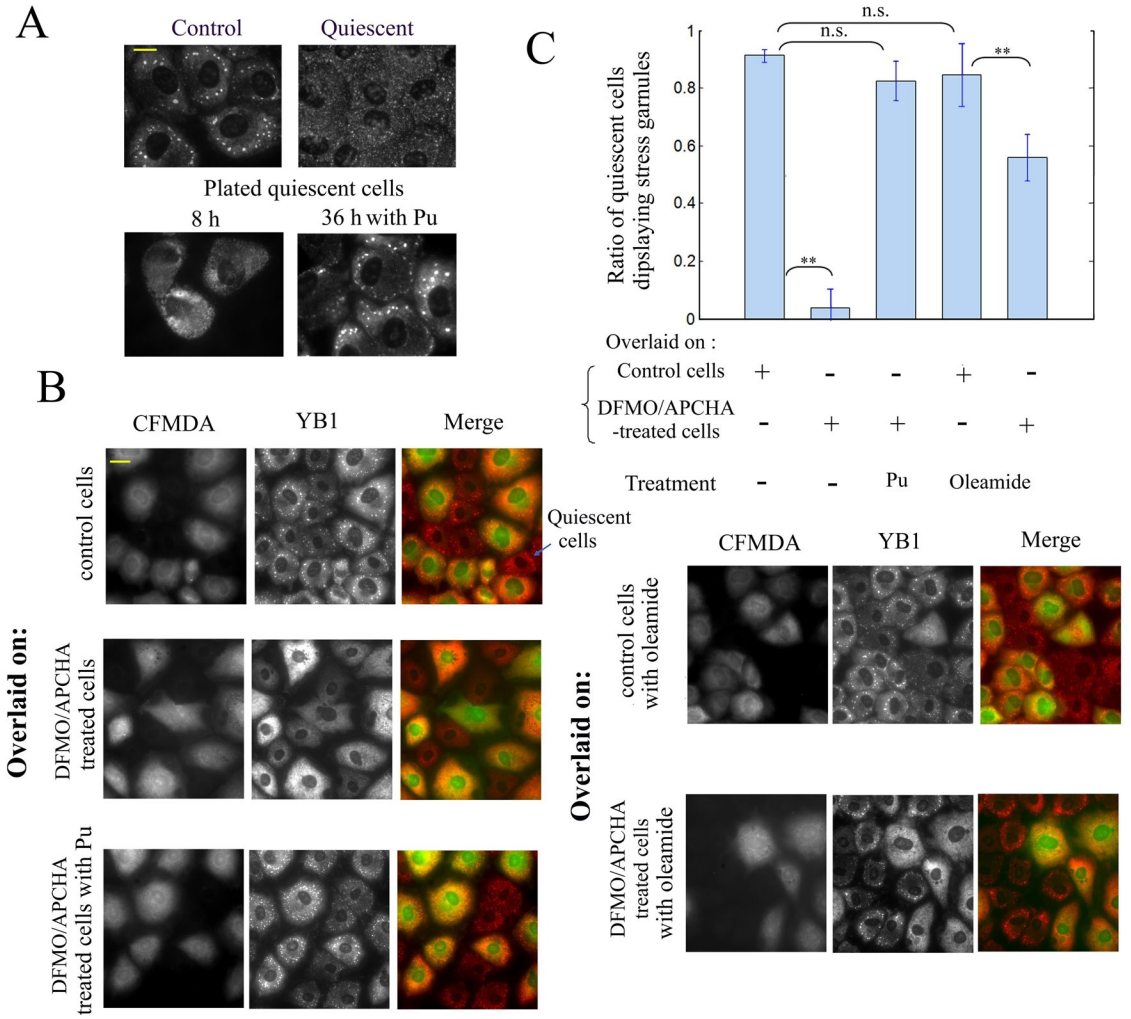

FIGURE 7: The formation of stress granules after arsenite exposure is impaired in quiescent cells but can be retrieved after interacting with control but not polyamine-depleted cells. (A) Stress granule assembly was analyzed after arsenite exposure (0.5 mM for 45 min) by anti-YB1 labeling in control, contact-inhibited quiescent cells and also in plated quiescent cells for 8 and 36 h. Quiescent cells can recover their ability to form normal stress granules 36 h after plating. Scale bar, 10 μm. (B) Quiescent cells were overlaid on subconfluent CFMDA-stained control or DFMO/APCHA-treated cells and allowed to interact for 36 h under indicated conditions without DFMO and APCHA. Stress granule formation was then observed after arsenite exposure. Quiescent cells do not form stress granules when overlaid on DFMO/APCHA-treated cells, but they recovered normal stress granule assembly after interacting with control cells. Putrescine supplementation (60 μM) allowed the recovery of stress granules in quiescent cells overlaid on DFMO/APCHA-treated cells. (C) Statistical measurements of stress granule formation in quiescent cells treated as in B. Note that oleamide allowed quiescent cells to form stress granules while interacting with polyamine-depleted cells. Scale bar, 15 μm. Results are mean ± SD from 600 cells on three different samples. *$p < 0.05$ by t test. n.s., not significant.

appearing upon arsenite exposure (Figure 7A). When quiescent cells were plated at low density (5×10^4 cells/cm^2), they retained their inability to form stress granules for 8 h after plating, compared with control cells plated under similar conditions (Supplemental Figure S8), but normal stress granules can be formed after 36 h when putrescine was present in the culture medium (Figure 7A). We may presume that quiescent cells replenished their polyamine pools, allowing the formation of stress granules after arsenite exposure.

Because DFMO/APCHA-treated cells can resume growth and retrieve the ability to form stress granules after interacting with control cells (Figure 6), we hypothesized that the intercellular interactions between DFMO/APCHA-treated and quiescent cells may not lead to the same outcome because quiescent cells have a low amount of polyamines (Table 1). To explore this idea, we overlaid quiescent cells onto control or DFMO/APCHA-treated cells and analyzed the formation of stress granules after 36 h (Figure 7, B and C). The results showed that polyamine-poor quiescent cells, when overlaid onto DFMO/APCHA-treated cells, cannot form granules and are unable to induce the formation of stress granules in DFMO/APCHA-treated cells but do form stress granules when overlaid on control cells. Of interest, oleamide allowed the partial recovery of stress granules in quiescent cells overlaid on DFMO/APCHA-treated cells (Figure 7, B and C). Gap junctions, which were observed in quiescent cells after plating (Supplemental Figure S9), could then lead to the inhibition of stress granule assembly in overlaid quiescent cells, possibly via the transit of polyamines to DFMO/APCHA-treated cells.

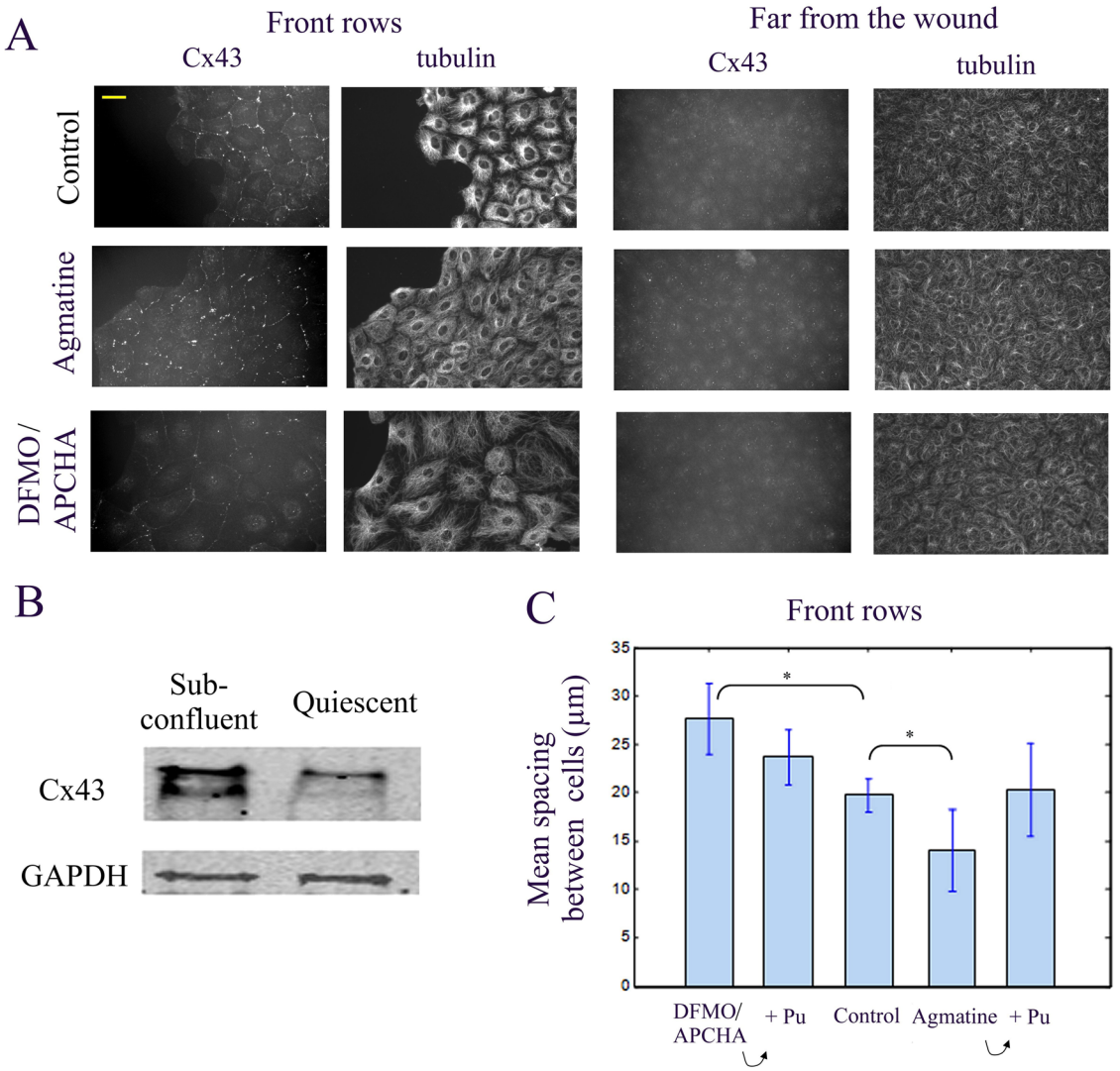

FIGURE 8: Microtubule and gap junction organization during wound healing in agmatine- and DFMO/APCHA-treated cells. (A) Monolayers of quiescent NRK cells were wounded using a surgical scalpel, and cells in the front rows or away for the wound were observed 6 d after indicated treatments. NRK cells were labeled with anti-tubulin and anti-Cx43. Agmatine and DFMO/APCHA treatments altered cell morphology in the front rows but were without effect on cells located far from the wound. Scale bar, 20 µm. (B) Representative Western blot from three experiments indicating that the Cx43 expression level is higher in subconfluent cells than in quiescent cells, which is in line with the low Cx43 staining observed in A in the quiescent state. GAPDH was used as a loading control. (C) Statistical measurements of the mean spacing between cells in the front rows revealed that cells were more compressed with agmatine than in control cells, in contrast with DFMO/APCHA treatment, which led to a larger spacing between cells. Results are mean ± SD from 500 cells on five different samples. *$p < 0.05$ by *t* test. n.s., not significant.

Wound healing results in an inhomogeneous distribution of stress granules in epithelia exposed to oxidative stress

Given that gap junction plaques are formed in the wounded zone (Spanakis *et al.*, 1998; Desforges *et al.*, 2011) and that migration of polyamine-depleted cells after DFMO treatment is generally impaired, with the inactivation of Rac1 as a possible explanation for this effect (Ray *et al.*, 2003), we explored whether there is a relationship between the variation in polyamine content between quiescent and proliferating cells and the variation in the occurrence of gap junctions in these cells during wound healing. In NRK cells, we observed that confluent quiescent cells did not display gap junction plaques (Figure 8A, right) and the expression of Cx43 was lower than in subconfluent cells (Figure 8B); quantification over three samples indicates that Cx43 expression after glyceraldehyde-3-phosphate dehydrogenase (GAPDH) normalization is reduced about three times (35 ± 10% compared with proliferating cells). In contrast, proliferating cells present in the front rows of migrating cells 6 d after the wound were densely gap junction–connected under control conditions. Similar results were obtained whether or not polyamines were present in the culture medium, which means that cells in the front rows were able to synthesize polyamines to promote their growth. When wound healing was performed on cells pretreated for 6 d with DFMO/APCHA, we observed a significant cell migration the first 3 d after the wound, as expected, since cells are able to divide the first days after DFMO/APCHA treatment (Nishimura *et al.*, 2005) and to migrate if DFMO is added during wounding (McCormack *et al.*, 1992), but both migration and proliferation were significantly reduced after 6 d. We also noticed that cells in the front

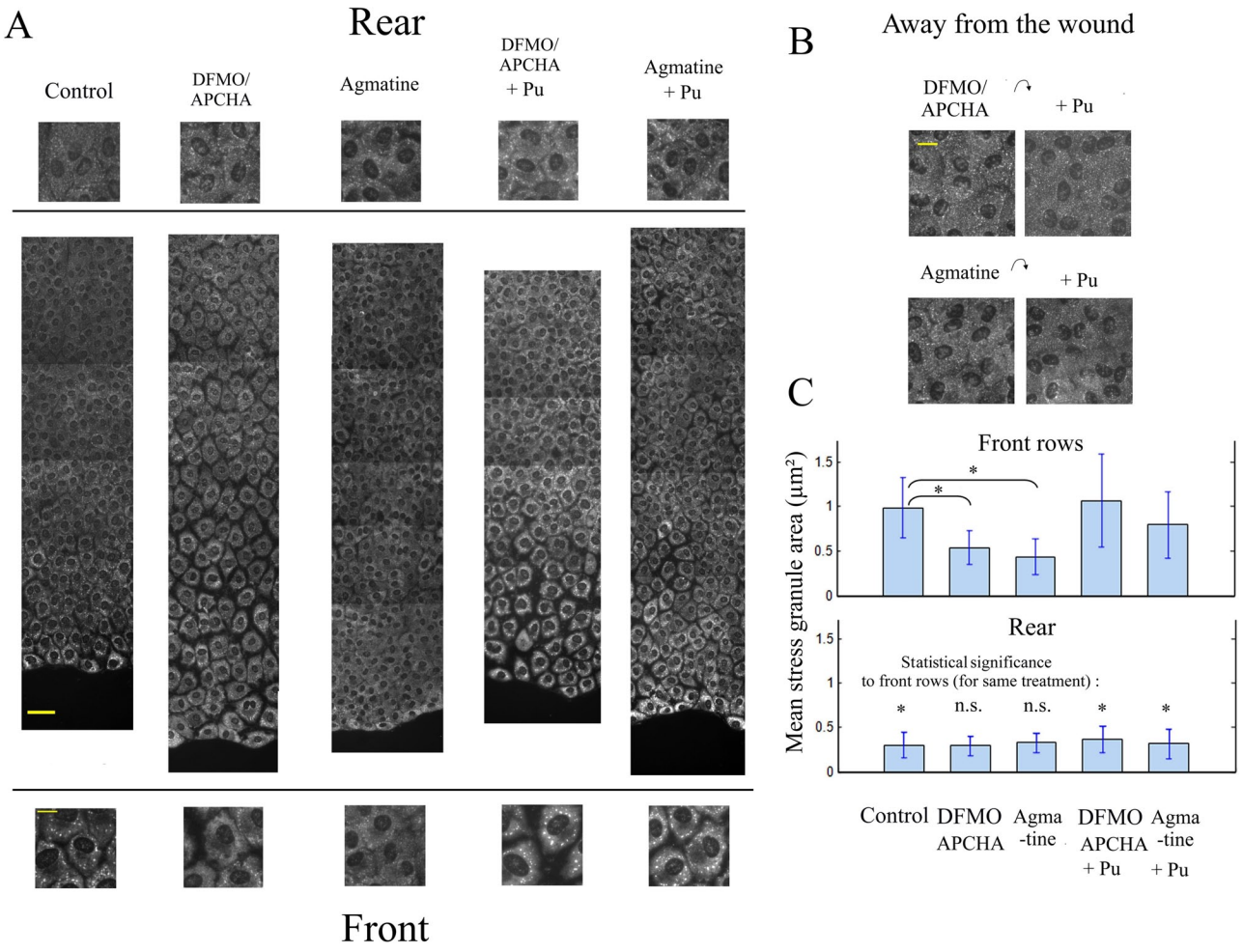

FIGURE 9: Wound healing leads to an inhomogeneous distribution of stress granules in epithelia after arsenite exposure. (A) Monolayers of quiescent NRK cells were wounded using a surgical scalpel, and cells from the leading edge to >1 mm from the wound were observed 6 d after indicated treatments. Cells were then exposed to 0.5 mM arsenite for 45 min to induce stress granule formation. Stress granules were detected with YB1 labeling. Cells located in the front rows, in both control and after putrescine supplementation, displayed large stress granules, whereas after both agmatine or DFMO/APCHA treatment, the formation of stress granules was impaired, with many small granules. Zooms represent cells located ~1 mm away the leading edge (rear) or in the front rows. Note that agmatine-treated cells were more compacted in the front rows, most probably due to the presence of many gap junctions. Scale bars, 30 μm, and 10 μm for zoom. (B) Far from the wound (>5 mm), the stress granules were smaller and less marked whatever the treatment, which may be linked to their quiescent state. Scale bar, 10 μm. (C) Statistical analysis of stress granule size after arsenite exposure in the front rows and away from the wound under indicated conditions. As noted earlier, stress granules were larger in the front rows than ~1 mm from the wound (rear), and polyamine depletion reduced stress granule size in the front rows. Results are mean ± SD from 800 granules. *$p < 0.05$ by *t* test. n.s., not significant.

rows spread on a larger area and displayed fewer gap junction plaques than control cells, a typical phenotype of subconfluent DFMO/APCHA-treated cells (Figure 8A). On the other hand, agmatine treatment led to the appearance of numerous gap junctions in the front rows, even more than in control cells. Furthermore, the cell morphology differs from that of subconfluent agmatine-treated cells (Supplemental Figure S1A), as no cell spreading was observed, but instead cells were even more compact in the front rows compared with control conditions (Figures 8C and 9A), which should be correlated with the presence of numerous gap junctions restraining cell migration (Qiu *et al.*, 2003). We then observed the formation of stress granules after arsenite treatment 6 d after wounding. The presence of stress granules was analyzed on sequential images at high resolution from the leading edge to >1 mm from the wound (Figure 9A). In control cells, large stress granules appear in the leading edge, whereas far from the wound, stress granule assembly was impaired, with many dot-like granules (Figure 9, B and C). In DFMO/APCHA-treated cells, stress granule assembly was impaired in the front rows but could be recovered by putrescine supplementation, which indicates that polyamine replenishment is necessary in the front rows for stress granule assembly. In agmatine-treated cells, we again observed densely packed cells in the front rows, but the formation of stress granules was also inhibited compared with control and restored by putrescine. A normal phenotype for agmatine-treated cells regarding cell density and stress granule formation can be restored by supplementation with putrescine. Taken together, these results indicate that an inhomogeneous distribution of polyamines appears during wound healing that parallels cell proliferation in the front rows

but also induces a differential translational response to oxidative stress from columnar quiescent cells in the epithelia.

DISCUSSION

A link between polyamines, the epithelial cell cytoskeleton, and gap junction communication

As a general rule, architecture plays a key role in promoting or preventing communication among individuals, and the spatial organization of mammalian cells, coordinated by the actin and microtubule networks, also needs to set the proper intercellular interactions with adjacent cells. In epithelial cells, which are under focus in the present study, cell architecture varies between quiescent and proliferative states. Quiescent epithelial cells generally display a typical columnar architecture, with stable microtubule bundles oriented along the basal apical axis (Bacallao *et al.*, 1989), whereas proliferating cells display centrosomal microtubules whose highly dynamical plus ends reach the cell periphery (Musch, 2004). In addition, and without reported correlation, a prerequisite to trigger cell proliferation is the presence of polyamines in sufficient amount (Heby, 1981; Kramer *et al.*, 2001). Quiescent epithelial cells have a significantly lower content of polyamines than do proliferating cells (Table 1) due to both the inhibition of polyamine synthesis and reduced polyamine uptake. In light of these facts, we may hypothesize that an increase in intracellular polyamine levels may enable the reorganization of the cytoskeleton when cells switch from quiescence to proliferation. Clues for such a possible relationship come from early reports showing that intracellular polyamine depletion leads to an impairment of cell migration, which could be attributed to the reorganization of the actin filament at the cell cortex via Rac1 inactivation (Ray *et al.*, 2003). The presence of thick actin fibers at the cell cortex acts as a barrier that tends to prevent migration and intercellular interaction. In addition, dynamical microtubules are less likely to cross this barrier in order to participate in the migration process and establish communications with adjacent cells. This pattern is reinforced by polyamine depletion, as it can impair microtubule assembly by decreasing the rate of incoming tubulin dimers at microtubule plus ends via facilitated diffusion (Mechulam *et al.*, 2009). Indeed, putrescine supplementation of polyamine-depleted cells increases microtubule elongation rates and the number of dynamical microtubule ends at the cell cortex (Figure 4). Although many parameters come into play to account for this architectural reorganization, transcription of growth-associated genes (Celano *et al.*, 1989), Rac1 activation, and microtubule regrowth make major contributions. The presence of dynamical microtubules at the cell cortex may then allow the transport of connexin proteins to the correct membrane location as EB1 targets gap junction plaques at the cell membrane (Shaw *et al.*, 2007), and a microtubule-binding domain has been identified in Cx43 (Giepmans *et al.*, 2001; Saidi Brikci-Nigassa *et al.*, 2012). This is supported, for example, by the observation that NRK cells treated with DFMO/APCHA displayed limited gap junction plaques at the cell/cell interface, whereas large gap junctions reappeared after putrescine supplementation, along with more intense Golgi trafficking (Figure 2); a similar pattern was observed for overlaid, polyamine-poor, quiescent cells after putrescine supplementation (Supplemental Figure S9). In addition to their beneficial effect on microtubule dynamics, polyamines may also increase Cx43 expression (Shore *et al.*, 2001). However, we found that agmatine treatment leads to Cx43 overexpression with long-range gap junction communication (Figure 2). Therefore the expression of Cx43 seems to depend on the means used to block natural polyamine synthesis. In the case of agmatine, it may mimic the high extracellular putrescine concentration used to obtain an overexpression of Cx43 (Shore *et al.*, 2001). The abnormally thick gap junction plaques observed in agmatine-treated cells most probably results from both Cx43 overexpression and the limited number of dynamical microtubule ends in polyamine-depleted cells (Figure 3), possibly through an inefficient withdrawal of nonfunctional Cx43 from existing gap junction plaques. Putrescine supplementation after agmatine treatment indeed allows the growth of dynamical microtubules and the recovery of normal gap junction plaques (Figures 2 and 4C).

Polyamines coordinate the cell response to stress in epithelial cells

Quiescent cells are less sensitive than cycling cells to many stresses such as oxidative stress (Lee *et al.*, 1996; Naderi *et al.*, 2003) and osmotic stress (Zhang *et al.*, 2002) partly because mRNA- and DNA-associated machinery works at slower rates than in proliferating cells. As a consequence, and some specific functions excepted, quiescent cells may not take advantage of communicating with proliferating cells, which are likely to spread toxic compounds (Lin *et al.*, 1998). On the other hand, cycling cells connected via gap junctions can propagate a death signal but can also mediate a coordinated response to stress, which may lead to a more positive outcome. For example, if all connected cells adopt the same appropriate strategy after oxidative stress, such as increased glutathione biosynthesis, a collective response would prevent a few cells to adopt the wrong defense strategy, which would spread toxic compound to adjacent cells and endanger all connected cells. To document such collective behavior, we analyzed the stress-induced reprogramming of the mRNA-associated machineries via stress granule formation (Kedersha *et al.*, 2005), which postpones the translation of housekeeping proteins while allowing that of stress-survival proteins like heat shock proteins. The point is that polyamines strongly influence the formation of stress granules (Li *et al.*, 2010), and stress granule assembly in polyamine-depleted NRK cells is impaired (Figure 6). By their action on stress granules, polyamines thus modulate the translational response among connected cells. In line with this, polyamine-depleted cells interacting with control cells recover the ability to form stress granules upon arsenite exposure, and such recovery is inhibited by blocking gap junction communications (Figure 6). More generally, polyamine-mediated interactions tend to maintain a coordinated response to stress among gap junction–connected cells (Figures 6 and 7), which is most probably linked to the similar proliferative status among connected cells. An interesting consequence is the inhomogeneous response to stress during wound healing (Figure 9). Proliferating cells in the front rows are polyamine rich, display dynamical microtubules and gap junction plaques at the cell cortex, and form stress granules, whereas those away from the wound are quiescent, polyamine poor, display no gap junction plaques, and do not from stress granules (Figure 8). The interaction of quiescent cells away from the wound with proliferating cells in the front rows thus does not inhibit stress granule assembly via passive diffusion of polyamines from proliferating polyamine-rich to polyamine-poor quiescent cells, most probably because quiescent NRK cells do not communicate via gap junctions.

Intercellular interaction mediated by polyamines and potential applications to control of cell proliferation in vivo

The control of cell proliferation in epithelia is a complex mechanism involving intracellular, intercellular, and many paracrine signals, such as growth factors (transforming growth factor [TGF], epidermal growth factor; Mendley and Toback, 1989; Gnecchi *et al.*, 2008). We propose that polyamines may contribute to growth control. Indeed when subconfluent NRK cells were treated with DFMO/APCHA for days, they

could no longer grow, even when DFMO and APCHA were washed out. To resume proliferation in the absence of extracellular polyamines, they need to interact with polyamine-rich control cells (Figure 5B). To explain this phenomenon, two hypotheses can be advanced: a transit of polyamines takes place from control to polyamine-depleted cells via gap junctions, and (or) control cells stimulate polyamine synthesis in polyamine-depleted cells. In line with the former hypothesis, the inhibition of gap junction communications significantly reduced the regrowth of polyamine-depleted cells interacting with control cells. In addition, the regrowth of polyamine-depleted cells is reduced but not stopped when polyamine synthesis is inhibited by DFMO during the interaction with control cells. However, polyamines transiting from control to polyamine-depleted cells may also trigger synthesis of polyamines in previously polyamine-depleted cells, leading to amplification of the polyamine-mediated signal, as observed in the absence of DFMO (Figure 5, B and C).

This polyamine-mediated intercellular signaling can provide further insight into in vivo processes. Here are some examples. 1) Nonproliferating liver cells display gap junctions and have a horizontal array of microtubules, in contrast with the vertical microtubule bundles in quiescent columnar NRK cells. During liver regeneration, a cyclical phase of gap junction disappearance and reappearance is generally observed. The disappearance coincides with DNA synthesis and is associated with a functional segregation of the replicating cells with adjacent cells (Dermietzel *et al.*, 1987). In this system, cells that resume cycling may have to block the passive diffusion of newly synthesized polyamines in adjacent, quiescent cells in order to increase their polyamine levels. 2) Polyamine-mediated gap junction communications can control growth in few connected cells, whereas other cells in close proximity can remain quiescent if they do not interact with them via gap junctions. Such localized control of growth could hardly be accomplished by diffusion of growth factors like TGF, which spread away from adjacent cells. 3) Because cancer cells generally display impaired gap junction communications (Yamasaki and Naus, 1996), the interaction between cancer and normal cells mediated by polyamines and its putative influence on cancer invasiveness deserve to be considered. In particular, because cancer cells have higher polyamine levels than normal cells, the loss of gap junction communication in cancer cells may prevent the transit of their polyamines to normal cells, allowing them to keep a high polyamine concentration and their high proliferation rate.

MATERIALS AND METHODS

Cell culture

NRK-52E cells (American Type Culture Collection, Manassas, VA) were grown in plastic dishes and maintained in DMEM supplemented with 5% (vol/vol) dialyzed fetal bovine serum (to remove exogenous polyamines), 2 mM L-glutamine, and 1% antibiotics (penicillin and streptomycin) in humidified 5% CO_2 atmosphere at 37°C. To deplete polyamines, cells were incubated for 6 d in the presence of a combination of 0.5 mM DFMO (Sigma-Aldrich, St. Louis, MO) and 100 µM APCHA (Alexis Biochemicals, San Diego, CA) or in the presence of 0.5 mM agmatine (Sigma-Aldrich). To analyze the effect of polyamine supplementation, polyamine-depleted cells were washed in phosphate-buffered saline (PBS) and incubated in the presence of 60 µM putrescine for the indicated times. To inhibit serum polyamine oxidase, 1 mM aminoguanidine was added to the culture medium.

Coculture assays

To distinguish between different cell populations, NRK cells were labeled with vital fluorescent dyes as follows: NRK cells after indicated treatment were incubated with 5 µM green 5-chloromethylfluorescein diacetate (CFMDA) or blue 7-amino-4-chloromethylcoumarin (CMAC) cell tracker, respectively (Molecular Probes, Eugene, OR) in serum-free DMEM for 20 min and washed extensively in PBS. When specified, NRK cells were trypsinized and overlaid on subconfluent DFMO/APCHA-treated or control cells (50,000 cells/cm^2) and then allowed to interact.

Scrape-loading experiments

Confluent but non–contact-inhibited NRK cells grown under specified treatments were rinsed twice in PBS. Lucifer yellow (LY), 30 µM (Sigma-Aldrich), a fluorescent dye used to evidence gap junction permeability, was then added to the PBS buffer. To load LY in cells, cells were scrapped using a surgical blade. After 4 min of incubation (required for the transfer of LY from cell to cell), the cells were washed twice with PBS, fixed with 4% paraformaldehyde (PFA) for 10 min, and mounted for fluorescence microscopy.

Wound-healing assay

NRK cells were grown to confluence and allowed to form monolayers of quiescent cells for 9 d. After scraping of the cell monolayers from one-half of the culture dishes (9.6 cm^2) using a surgical blade, the process of wound healing was allowed to take place for 6 d under indicated conditions.

Immunoblotting

Cells were lysed in 50 mM Tris-HCl (pH 7.5), 150 mM NaCl, 0.1% (vol/vol) Triton X-100, 1 mM EDTA, and protease inhibitor cocktail (Roche, Indianapolis, IN). Lysates were centrifuged at 14,000 × *g* for 15 min at 4°C, and supernatants were collected. Proteins were separated on 12% SDS–PAGE gels and transferred onto a nitrocellulose membrane (Invitrogen, Carlsbad, CA). The membranes were blocked in 5% (wt/vol) nonfat dried milk/PBS for 30 min at room temperature and incubated for 1 h at room temperature with primary antibodies (anti-Cx43; 1:2000 dilution; Abcam, Cambridge, MA) and anti-GAPDH used as a protein loading control (1:5000; Abcam). Bound antibodies were detected and quantified with an Odyssey imaging system (LI-COR Biosciences, Lincoln, NE) using anti-rabbit IRDye 800 or anti-mouse IRDye 680 secondary antibodies (1:5000 dilution; Odyssey; LI-COR Biosciences).

Immunofluorescence

After indicated treatments, NRK cells growing in plastic dishes were washed with PBS and fixed with 4% PFA in PBS for 15 min at 37°C. Cells were permeabilized with 0.5% Triton X-100 for 15 min and then washed and incubated for 1 h in blocking solution (50 mM Tris-HCl, 150 mM NaCl, 0.1% [vol/vol] Triton X-100, 2% bovine serum albumin, pH 7.5) with a rabbit anti–YB-1 polyclonal antibody (produced as described in Davydova *et al.*, 1997), a mouse monoclonal anti-tubulin antibody (clone tub 2.1, 1:5000), a rabbit anti-Cx43 (1:1000; Abcam), or a mouse anti-EB1 (1:1000; BD Biosciences, San Diego, CA). Cells were washed extensively in PBS and incubated for 2 h with secondary antibodies (Alexa Fluor 488 and Alexa Fluor 555, 1:2500 dilution, or rhodamine-labeled phalloidin, 1:1000 [Molecular Probes]) in blocking solution. After final washes with PBS, cell grown on plastic were covered with glass coverslips to proceed for fluorescence microscopy. For the statistics, the mean granule area was measured using ImageJ (National Institutes of Health, Bethesda, MD) software over at least 800 granules from at least 10 different representative cells. Because stress granules are not round, the apparent radii were not considered. Spacing between cells was estimated by locating the nucleus center of mass and measuring at

least 500 separating distances between nearest neighbors with the ImageJ software.

BrdU immunofluorescence

BrdU (60 μM) was added to the buffer for the last 6 h of the indicated treatments. NRK cells were then fixed with cold methanol for 10 min (–20°C), rinsed twice with PBS, and fixed again with 4% PFA for 15 min at room temperature. After two PBS washes, cells were permeabilized with 0.5% (vol/vol) Triton X-100 in PBS for 1 h, denatured in 2 N HCl for 20 min, rinsed twice in PBS, and incubated overnight with goat anti-BrdU (Abcam) in blocking solution. Cells were rinsed in PBS, incubated for 2 h with secondary antibodies, and rinsed in PBS. Finally, cells were prepared for fluorescence microscopy.

Intracellular polyamine quantification

Polyamine levels were quantified according to a modification of the method of Loukou and Zotou (2003) by dansyl derivatization and ion-paired reverse-phase high-pressure liquid chromatography using fluorometric detection. In brief, samples (3 mg/ml protein from NRK cell extracts) were centrifuged at 3000 × *g* for 5 min. Then 25 μl of supernatants was homogenized with borate buffer (0.4 M, pH 9, 2 ml) and incubated for 90 min at 100°C in the dark with 0.5 ml of dansyl chloride (5 mg/ml in acetone). Dansyl derivatives were purified by solid-phase extraction (Bond Elut Certify cartridge; Agilent Technologies, Santa Clara, CA). The organic phase was collected and evaporated, and the dansyl derivatives were resuspended in 1 ml of the initial mobile phase. The separation of dansyl-putrescine, dansyl-spermidine, and dansyl-spermine was performed on a C18 Luna column (length 25 cm, particle diameter 5 μm; Phenomenex, Torrance, CA) using an acetonitrile/water gradient on a Dionex system (Thermo Scientific, Waltham, MA) for fluorometric detection. Polyamine concentrations were estimated by the internal standard method (standard: hexane diamine). In parallel, a 10-μl aliquot of the cell suspension was used to quantify by hemacytometry the number of cells analyzed by chromatography. This allowed us to express the results as femtomoles per cell. The reported values are averages of three different samples for each condition. The error represents the SD from the mean.

Videomicroscopy of microtubule dynamics

NRK cells were transiently transfected with a green fluorescent protein (GFP)–EB1 eukaryotic expression vector and then cultured for 24 h before real-time monitoring of microtubule dynamics. Fluorescence videomicroscopy was implemented on an inverted microscope (Axiovert 220; Carl Zeiss MicroImaging, Jena, Germany). GFP emission was detected with a 63×/1.4 numerical aperture objective. Time-lapse images were captured at 4-s intervals using a Zeiss cooled charge-coupled device camera. To measure microtubule elongation rates, the distances covered by microtubule ends were measured by analyzing sequential images with the ImageJ software. Ambiguous trajectories were discarded. See Supplemental Videos S1–S3.

ACKNOWLEDGMENTS

This work was supported by funds from the Institut National de la Santé et de la Recherche Médicale, the Genopole Evry, and an ANR grant (NAFLD-Citrulline).

REFERENCES

Arimoto K, Fukuda H, Imajoh-Ohmi S, Saito H, Takekawa M (2008). Formation of stress granules inhibits apoptosis by suppressing stress-responsive MAPK pathways. Nat Cell Biol 10, 1324–1332.

Bacallao R, Antony C, Dotti C, Karsenti E, Stelzer EH, Simons K (1989). The subcellular organization of Madin-Darby canine kidney cells during the formation of a polarized epithelium. J Cell Biol 109, 2817–2832.

Bello-Fernandez C, Packham G, Cleveland JL (1993). The ornithine decarboxylase gene is a transcriptional target of c-Myc. Proc Natl Acad Sci USA 90, 7804–7808.

Beppu T, Shirahata A, Takahashi N, Hosoda H, Samejima K (1995). Specific depletion of spermidine and spermine in HTC cells treated with inhibitors of aminopropyltransferases. J Biochem 117, 339–345.

Casero RA Jr, Pegg AE (1993). Spermidine/spermine N1-acetyltransferase—the turning point in polyamine metabolism. FASEB J 7, 653–661.

Celano P, Baylin SB, Casero RA Jr (1989). Polyamines differentially modulate the transcription of growth-associated genes in human colon carcinoma cells. J Biol Chem 264, 8922–8927.

Celano P, Baylin SB, Giardiello FM, Nelkin BD, Casero RA Jr (1988). Effect of polyamine depletion on c-myc expression in human colon carcinoma cells. J Biol Chem 263, 5491–5494.

Chernov KG, Barbet A, Hamon L, Ovchinnikov LP, Curmi PA, Pastre D (2009). Role of microtubules in stress granule assembly: microtubule dynamical instability favors the formation of micrometric stress granules in cells. J Biol Chem 284, 36569–36580.

Coffino P (2001). Regulation of cellular polyamines by antizyme. Nat Rev Mol Cell Biol 2, 188–194.

Davydova EK, Evdokimova VM, Ovchinnikov LP, Hershey JW (1997). Overexpression in COS cells of p50, the major core protein associated with mRNA, results in translation inhibition. Nucleic Acids Res 25, 2911–2916.

Dermietzel R, Yancey SB, Traub O, Willecke K, Revel JP (1987). Major loss of the 28-kD protein of gap junction in proliferating hepatocytes. J Cell Biol 105, 1925–1934.

Desforges B, Savarin P, Bounedjah O, Delga S, Hamon L, Curmi PA, Pastre D (2011). Gap junctions favor normal rat kidney epithelial cell adaptation to chronic hypertonicity. Am J Physiol Cell Physiol 301, C705–C716.

el-Fouly MH, Trosko JE, Chang CC (1987). Scrape-loading and dye transfer. A rapid and simple technique to study gap junctional intercellular communication. Exp Cell Res 168, 422–430.

Gabbiani G, Chaponnier C, Huttner I (1978). Cytoplasmic filaments and gap junctions in epithelial cells and myofibroblasts during wound healing. J Cell Biol 76, 561–568.

Giepmans BN, Verlaan I, Hengeveld T, Janssen H, Calafat J, Falk MM, Moolenaar WH (2001). Gap junction protein connexin-43 interacts directly with microtubules. Curr Biol 11, 1364–1368.

Gnecchi M, Zhang Z, Ni A, Dzau VJ (2008). Paracrine mechanisms in adult stem cell signaling and therapy. Circ Res 103, 1204–1219.

Goliger JA, Paul DL (1995). Wounding alters epidermal connexin expression and gap junction-mediated intercellular communication. Mol Biol Cell 6, 1491–1501.

Guan X, Cravatt BF, Ehring GR, Hall JE, Boger DL, Lerner RA, Gilula NB (1997). The sleep-inducing lipid oleamide deconvolutes gap junction communication and calcium wave transmission in glial cells. J Cell Biol 139, 1785–1792.

Heby O (1981). Role of polyamines in the control of cell proliferation and differentiation. Differentiation 19, 1–20.

Heby O, Marton LJ, Zardi L, Russell DH, Baserga R (1975). Changes in polyamine metabolism in WI38 cells stimulated to proliferate. Exp Cell Res 90, 8–14.

Heby O, Sarna GP, Marton LJ, Omine M, Perry S, Russell DH (1973). Polyamine content of AKR leukemic cells in relation to the cell cycle. Cancer Res 33, 2959–2964.

Jakus J, Wolff EC, Park MH, Folk JE (1993). Features of the spermidine-binding site of deoxyhypusine synthase as derived from inhibition studies. Effective inhibition by bis- and mono-guanylated diamines and polyamines. J Biol Chem 268, 13151–13159.

Kedersha N, Stoecklin G, Ayodele M, Yacono P, Lykke-Andersen J, Fritzler MJ, Scheuner D, Kaufman RJ, Golan DE, Anderson P (2005). Stress granules and processing bodies are dynamically linked sites of mRNP remodeling. J Cell Biol 169, 871–884.

Kramer DL, Chang BD, Chen Y, Diegelman P, Alm K, Black AR, Roninson IB, Porter CW (2001). Polyamine depletion in human melanoma cells leads to G1 arrest associated with induction of p21WAF1/CIP1/SDI1, changes in the expression of p21-regulated genes, and a senescence-like phenotype. Cancer Res 61, 7754–7762.

Kwon H, Ford SP, Bazer FW, Spencer TE, Nathanielsz PW, Nijland MJ, Hess BW, Wu G (2004). Maternal nutrient restriction reduces concentrations of amino acids and polyamines in ovine maternal and fetal plasma and fetal fluids. Biol Reprod 71, 901–908.

Landau G, Bercovich Z, Park MH, Kahana C (2010). The role of polyamines in supporting growth of mammalian cells is mediated through their requirement for translation initiation and elongation. J Biol Chem 285, 12474–12481.
Lauf U, Giepmans BN, Lopez P, Braconnot S, Chen SC, Falk MM (2002). Dynamic trafficking and delivery of connexons to the plasma membrane and accretion to gap junctions in living cells. Proc Natl Acad Sci USA 99, 10446–10451.
Lee PJ, Alam J, Wiegand GW, Choi AM (1996). Overexpression of heme oxygenase-1 in human pulmonary epithelial cells results in cell growth arrest and increased resistance to hyperoxia. Proc Natl Acad Sci USA 93, 10393–10398.
Li CH, Ohn T, Ivanov P, Tisdale S, Anderson P (2010). eIF5A promotes translation elongation, polysome disassembly and stress granule assembly. PLoS One 5, e9942.
Lin JH, Weigel H, Cotrina ML, Liu S, Bueno E, Hansen AJ, Hansen TW, Goldman S, Nedergaard M (1998). Gap-junction-mediated propagation and amplification of cell injury. Nat Neurosci 1, 494–500.
Lortie MJ, Novotny WF, Peterson OW, Vallon V, Malvey K, Mendonca M, Satriano J, Insel P, Thomson SC, Blantz RC (1996). Agmatine, a bioactive metabolite of arginine. Production, degradation, and functional effects in the kidney of the rat. J Clin Invest 97, 413–420.
Loukou Z, Zotou A (2003). Determination of biogenic amines as dansyl derivatives in alcoholic beverages by high-performance liquid chromatography with fluorimetric detection and characterization of the dansylated amines by liquid chromatography-atmospheric pressure chemical ionization mass spectrometry. J Chromatogr A 996, 103–113.
McCormack SA, Ray RM, Blanner PM, Johnson LR (1999). Polyamine depletion alters the relationship of F-actin, G-actin, and thymosin beta4 in migrating IEC-6 cells. Am J Physiol 276, C459–468.
McCormack SA, Viar MJ, Johnson LR (1992). Migration of IEC-6 cells: a model for mucosal healing. Am J Physiol 263, G426–G435.
McCormack SA, Viar MJ, Johnson LR (1993). Polyamines are necessary for cell migration by a small intestinal crypt cell line. Am J Physiol 264, G367–G374.
Mechulam A, Chernov KG, Mucher E, Hamon L, Curmi PA, Pastre D (2009). Polyamine sharing between tubulin dimers favours microtubule nucleation and elongation via facilitated diffusion. PLoS Comput Biol 5, e1000255.
Mendley SR, Toback FG (1989). Autocrine and paracrine regulation of kidney epithelial cell growth. Annu Rev Physiol 51, 33–50.
Meyskens FL Jr, Gerner EW (1999). Development of difluoromethylornithine (DFMO) as a chemoprevention agent. Clin Cancer Res 5, 945–951.
Moinard C, Cynober L, de Bandt JP (2005). Polyamines: metabolism and implications in human diseases. Clin Nutr 24, 184–197.
Musch A (2004). Microtubule organization and function in epithelial cells. Traffic 5, 1–9.
Naderi J, Hung M, Pandey S (2003). Oxidative stress-induced apoptosis in dividing fibroblasts involves activation of p38 MAP kinase and over-expression of Bax: resistance of quiescent cells to oxidative stress. Apoptosis 8, 91–100.
Nishimura K, Murozumi K, Shirahata A, Park MH, Kashiwagi K, Igarashi K (2005). Independent roles of eIF5A and polyamines in cell proliferation. Biochem J 385, 779–785.
Nishimura K, Ohki Y, Fukuchi-Shimogori T, Sakata K, Saiga K, Beppu T, Shirahata A, Kashiwagi K, Igarashi K (2002). Inhibition of cell growth through inactivation of eukaryotic translation initiation factor 5A (eIF5A) by deoxyspergualin. Biochem J 363, 761–768.
Pegg AE (2009). Mammalian polyamine metabolism and function. IUBMB Life 61, 880–894.
Pepper MS, Spray DC, Chanson M, Montesano R, Orci L, Meda P (1989). Junctional communication is induced in migrating capillary endothelial cells. J Cell Biol 109, 3027–3038.
Qiu C, Coutinho P, Frank S, Franke S, Law LY, Martin P, Green CR, Becker DL (2003). Targeting connexin43 expression accelerates the rate of wound repair. Curr Biol 13, 1697–1703.
Ray RM, McCormack SA, Covington C, Viar MJ, Zheng Y, Johnson LR (2003). The requirement for polyamines for intestinal epithelial cell migration is mediated through Rac1. J Biol Chem 278, 13039–13046.
Russell DH, Russell SD (1975). Relative usefulness of measuring polyamines in serum, plasma, and urine as biochemical markers of cancer. Clin Chem 21, 860–863.
Saidi Brikci-Nigassa A, Clement MJ, Ha-Duong T, Adjadj E, Ziani L, Pastre D, Curmi PA, Savarin P (2012). Phosphorylation controls the interaction of the connexin43 C-terminal domain with tubulin and microtubules. Biochemistry 51, 4331–4342.
Satriano J, Isome M, Casero RAJr, Thomson SC, Blantz RC (2001). Polyamine transport system mediates agmatine transport in mammalian cells. Am J Physiol Cell Physiol 281, C329–C334.
Satriano J, Matsufuji S, Murakami Y, Lortie MJ, Schwartz D, Kelly CJ, Hayashi S, Blantz RC (1998). Agmatine suppresses proliferation by frameshift induction of antizyme and attenuation of cellular polyamine levels. J Biol Chem 273, 15313–15316.
Savarin P *et al*. (2010). A central role for polyamines in microtubule assembly in cells. Biochem J 430, 151–159.
Seiler N, Delcros JG, Moulinoux JP (1996). Polyamine transport in mammalian cells. An update. Int J Biochem Cell Biol 28, 843–861.
Shaw RM, Fay AJ, Puthenveedu MA, von Zastrow M, Jan YN, Jan LY (2007). Microtubule plus-end-tracking proteins target gap junctions directly from the cell interior to adherens junctions. Cell 128, 547–560.
Shipe JR Jr, Hunt DF, Savory J (1979). Plasma polyamines determined by negative-ion chemical ionization/mass spectrometry. Clin Chem 25, 1564–1571.
Shore L, McLean P, Gilmour SK, Hodgins MB, Finbow ME (2001). Polyamines regulate gap junction communication in connexin 43-expressing cells. Biochem J 357, 489–495.
Spanakis SG, Petridou S, Masur SK (1998). Functional gap junctions in corneal fibroblasts and myofibroblasts. Invest Ophthalmol Vis Sci 39, 1320–1328.
Tabor CW, Tabor H (1984). Polyamines. Annu Rev Biochem 53, 749–790.
Tapon N, Hall A (1997). Rho, Rac and Cdc42 GTPases regulate the organization of the actin cytoskeleton. Curr Opin Cell Biol 9, 86–92.
Thomas T, Thomas TJ (2001). Polyamines in cell growth and cell death: molecular mechanisms and therapeutic applications. Cell Mol Life Sci 58, 244–258.
van Zoelen EJ, Tertoolen LG (1991). Transforming growth factor-beta enhances the extent of intercellular communication between normal rat kidney cells. J Biol Chem 266, 12075–12081.
Veenstra RD (1996). Size and selectivity of gap junction channels formed from different connexins. J Bioenerg Biomembr 28, 327–337.
Watanabe S, Kusama-Eguchi K, Kobayashi H, Igarashi K (1991). Estimation of polyamine binding to macromolecules and ATP in bovine lymphocytes and rat liver. J Biol Chem 266, 20803–20809.
Weber PA, Chang HC, Spaeth KE, Nitsche JM, Nicholson BJ (2004). The permeability of gap junction channels to probes of different size is dependent on connexin composition and permeant-pore affinities. Biophys J 87, 958–973.
Witte MB, Barbul A (2003). Arginine physiology and its implication for wound healing. Wound Repair Regen 11, 419–423.
Yamasaki H, Naus CC (1996). Role of connexin genes in growth control. Carcinogenesis 17, 1199–1213.
Zhang Z, Cai Q, Michea L, Dmitrieva NI, Andrews P, Burg MB (2002). Proliferation and osmotic tolerance of renal inner medullary epithelial cells in vivo and in cell culture. Am J Physiol Renal Physiol 283, F302–F308.